Polarized Raman scattering from single GaN nanowires

Tsachi Livneh,[1,*] Jinping Zhang,[2] Guosheng Cheng,[1] and Martin Moskovits[1,†]
[1]*Department of Chemistry and Biochemistry, University of California, Santa Barbara, California 93106-9510, USA*
[2]*Department of Materials Engineering, University of California, Santa Barbara, California 93106-9510, USA*
(Received 2 January 2005; revised manuscript received 6 March 2006; published 14 July 2006)

Raman spectra of single (hexagonal wurtzite) GaN nanowires grown by vapor-liquid-solid synthesis were recorded. By investigating the polarization dependence of the Raman intensities of the observed bands as a function of the angle between the long axis of the nanowire and the electric vector of the incident (and scattered) light, one is able to distinguish between nanowires whose crystallographic *c* axis corresponds to (c^* directed), or is substantially perpendicular to (a^* directed) the long axis of the nanowire—the two preferred directions of nanowire growth. For a^*-directed nanowires, polarization-dependent Raman intensity analysis can also determine, within tolerable limits, the orientation of the crystalline *c* axis with respect to laboratory-fixed coordinates. Simultaneous transmission electron microscopy (TEM) analyses confirm the conclusions derived from the Raman measurements. The polarization-dependent Raman intensities could only be understood if one assumed a complex-valued Raman tensor. The detection of resonance enhancement together with the tendency of the nanowires to grow with a high concentration of defects and the observation of yellow luminescence in the photoluminescence spectrum may account for the complex-valued Raman tensor we observe for GaN even at sub-band-gap photon energies.

DOI: 10.1103/PhysRevB.74.035320 PACS number(s): 63.22.+m

I. INTRODUCTION

Nanoscience is currently at the threshold of being able to incorporate nanostructures fabricated using so-called bottom-up techniques into workable devices,[1] including nanodevices based on GaN nanowires.[2] Accordingly, it is essential to develop *in situ* techniques for probing the morphology and other properties of nanostructures, such as nanowires, as circuit elements, or as building blocks for single nanowire photonics.[3] This is because many of the most powerful synthetic techniques, such as chemical vapor deposition (CVD) produce a range of structures. And while ideally one wishes either to restrict the synthesis to the desired nanowire geometry or, at least, to be able to select at the outset the desired form from among the distribution of structures, this is not always possible. For highly crystalline structures, high-resolution transmission electron microscopy (TEM) both as an imaging and as a diffractive instrument, can normally determine structure unambiguously. However, TEM is hard to apply *in situ*.

In this report we discuss the use of polarized Raman spectroscopy to determine the structure of single GaN nanowires, comparing the geometrical information obtained from the Raman polarization data with structural information obtained from high-resolution TEM. In particular we examine the sensitivity of the Raman spectrum to the relative orientation of the *k* vector and electric vector of the incident and scattered light with respect to the crystallographic axes of the single-crystalline material comprising the nanowire and the disposition of the crystal axes with respect to the long axis defining the nanowire. Because our GaN nanowires absorb in the wavelength regime used (514.5 nm), the Raman susceptibility tensor elements are complex valued. This enriches the angle dependence of the polarized Raman spectrum, allowing the relative phases among the Raman tensor elements (of some bands) to be determined, as was previously shown by Starch *et al.* in thin-film $SmBa_2Cu_3O_{7-\delta}$ (Ref. 4) and compared to first principle calculations on $YBa_2Cu_3O_{7-\delta}$.[5] Several Raman studies of GaN are extant,[6–10] including one of a GaN nanowire,[11–13] as well as of other nanowires, including Si (Refs. 14 and 15) and GaP,[16] and of carbon nanotubes (down to single walled).[17,18] Other than a recent study of CuO nanorods[19] involving polarized Raman, the potential of Raman spectroscopy as a nanowire structure-determination tool is essentially unexplored.

II. EXPERIMENTAL

Nanowires were synthesized in indium nanodroplets formed on an alumina substrate as described in Ref. 20. Sonicating the alumina substrate briefly in isopropanol released and dispersed single nanowires, which could then be deposited on TEM grids. The TEM grids were placed on a hollow holder in order to avoid contributions from light that is back-reflected from the surface underneath the grid. Raman spectra, excited with argon ion laser light (514.5 nm) and dispersed on a 1200 grooves/mm grating, were recorded in a back-scattering geometry using a Dilor LabRam micro-Raman spectrometer. After focusing with a 100× (0.8 NA) lens the typical power at the nanowire was 10^3–10^4 W/cm^2. The polarization vector was rotated using a half-wave plate positioned such that both the incident and backscattered light passed through the plate. Hence the electric vector of the parallel component (denoted as ∥) of the scattered light was coincident in direction with that of the incident light. This component as well as the so-called perpendicular component (denoted as ⊥) was selected out of the scattered signal with an analyzing polarizer situated between the half-wave plate and the spectrometer. In order to simplify the measurements and the transformation from laboratory coordinates to crystal-fixed coordinates,[21] the origin of the laboratory-fixed coordinates were chosen such that the long axis of the nano-

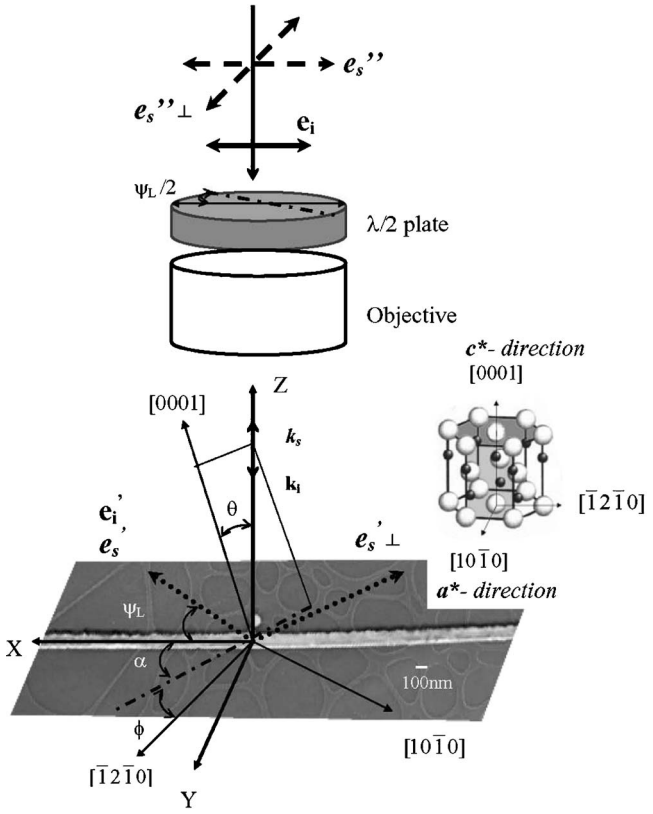

FIG. 1. Backscattering experimental geometry. The incoming light (e_i) directed along the Z axis passes through a $\lambda/2$ plate and a $100\times$ objective (0.8 NA) and reaches the nanowire at an angle ψ_L (e_i') with respect to its principle axis (X). The light scattered at angle ψ_S is analyzed as either a parallel (e_s') or a perpendicular ($e_s'^{\perp}$) component, rotated back to e_s'' ($\equiv e_i$) (∥) or $e_s''^{\perp}$ ($\equiv e_i+90^{\circ}$) (⊥), respectively. θ is the inclination of the c axis with respect to the Z axis, the (laboratory-fixed) normal to the substrate. Inset: GaN wurtzite structure (Ga=gray circles and N=black circles) with the $(10\bar{1}0)$ and (0001) planes denoted in light gray and dark gray, respectively.

wire lay along one of the canonical lab directions (the X direction). Likewise, the crystal-fixed coordinates were defined such that the x, y, and z axes are aligned along the $[10\bar{1}0]$, $[\bar{1}2\bar{1}0]$, $[0001]$ crystallographic directions. The relationships between the various axes and the polarization vectors are shown in Fig. 1.

III. RESULTS AND DISCUSSIONS

GaN crystallizes in the (hexagonal) wurtzite structure (space group $C_{6v}{}^4$-$P6_3mc$) with two formula units per primitive cell.[6,7] This is shown as an inset to Fig. 1 where the $(10\bar{1}0)$ and (0001) planes, are denoted with light and dark gray colors, respectively. The as-synthesized nanowires were found by TEM analysis to occur primarily (but not exclusively) in two forms: one with the unique $[0001]$ crystal axis (the c axis) coincident with the long axis of the nanowire. We will refer to these as c^*-directed nanowires since they along the normal of the (0001) plane, and one in which the $[10\bar{1}0]$ axis lies along the long axis of the nanowire. These correspond to the a^*-directed nanowires since they grow along the normal of the $(10\bar{1}0)$ plane. In a^*-directed nanowires, the c axis is perpendicular to the long axis of the nanowire. Obviously, c^*-directed nanowires are (optically) cylindrically symmetric, while a^*-directed nanowires are not. Hence, the Raman spectrum of a c^*-directed nanowire lying on a substrate is expected to be independent of rotations about the nanowire's long axis, while that of an a^*-directed nanowire will depend critically on the relative disposition of the nanowire's c axis with respect to the (laboratory-fixed) normal to the substrate on which it rests.

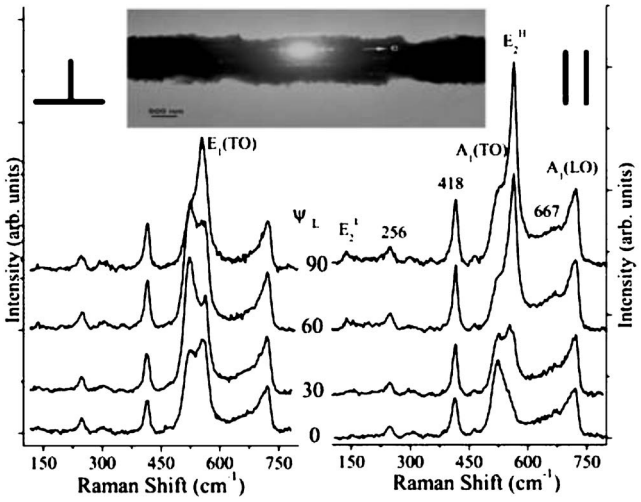

FIG. 2. A series of parallel (∥) and perpendicularly (⊥) polarized Raman spectra measured as a function of the polarization direction of the incident light for a 500 nm diameter nanowire shown by electron diffraction (TEM) to be c^* directed.

Group theory predicts four Raman active modes:[6,7] A_1, E_1, $2E_2$ (E_2^L and E_2^H). The A_1 and E_1 are polar modes: i.e., the interaction of the vibration with the long-range Coulomb field leads to energy differences between phonons polarized longitudinally and transverse to the direction of propagation of the phonon. The A_1 and E_1 modes are therefore split into LO and TO modes. Figure 2 shows a series of parallel and perpendicularly polarized Raman spectra measured as a function of the polarization direction of the incident light for a 500 nm diameter nanowire shown by electron diffraction (TEM) to be c^* directed. The nanowire's c axis lies along the X axis.

The peaks at 143, 556, 568, and 724 cm^{-1} are assigned to first-order phonons of E_2^L, E_1(TO), E_2^H,[6,7] and A_1(LO),[11–13] respectively. Assigning the 525 cm^{-1} is more difficult: Its symmetry properties are clearly those of the A_1(TO) mode (the c axis is perpendicular to the phonon propagation direction) but its energy is red shifted by ~8 cm^{-1} from its bulk value (as reported in Ref. 13 but unlike what Refs. 11 and 12 report). The profile of this band could not be fitted with a Lorentzian unless an additional band at ~533 cm^{-1} was assumed to be present with a polarization dependence that resembles that of the 525 cm^{-1} band. The frequency shift might be attributable to the formation of coupled plasmon-phonon mode (PLP), which is found in systems with high

carrier concentrations.[22] In that case, however, the polarization behavior should be that of an A_1(LO) mode[22] and we therefore consider this assignment unlikely. Finally, three additional bands are observed: at 418 cm^{-1} with an incident polarization dependence that resembles that of the A_1(LO) mode, a band at 256 cm^{-1} that also shows very little polarization dependence, and a band at 667 cm^{-1} that was assigned to vacancy-related defects.[6]

The relative intensities of the various bands can be calculated from the corresponding Raman tensors recalling that, in general, the tensor components will be complex valued. This fact is generally ignorable when the illuminating laser is polarized so that its electric vector lies along one of the principal crystallographic axes since in that configuration the inner product [Eq. (1)] will pick out only a single tensor element whose phase vanishes when the modulus is taken. Because in this study we vary $\psi_{L,S}$, the angle between the polarization vector of the incident and scattered light (which are coincident for our experimental configuration) and the long axis of the nanowire [which coincides with the (laboratory-fixed) X axis], the Raman intensity will, in some cases, depend on the relative values of the phases of the tensor components involved.

The forms of the Raman tensor, $\overleftrightarrow{R}$, for the pertinent phonon symmetries are as follows:

$$\overleftrightarrow{R}(A_1)=\begin{bmatrix} a & & \\ & a & \\ & & c \end{bmatrix} \quad \overleftrightarrow{R}_1(E_2)=\begin{bmatrix} d & & \\ & -d & \\ & & \end{bmatrix} \quad \overleftrightarrow{R}_1(E_1)=\begin{bmatrix} & & e \\ & & \\ e & & \end{bmatrix}$$

$$\overleftrightarrow{R}_2(E_2)=\begin{bmatrix} & -d & \\ -d & & \\ & & \end{bmatrix} \quad \overleftrightarrow{R}_2(E_1)=\begin{bmatrix} & & e \\ & & \\ & e & \end{bmatrix}.$$

The observed Raman intensity for the jth phonon is proportional to

$$I_j \sim |\hat{e}_s \cdot \overleftrightarrow{R}_j(\omega_L) \cdot \hat{e}_l|^2, \tag{1}$$

where $\hat{e}_{l,s}$ represent unit vectors in the incident (l) and scattered (s) directions, respectively. In the backscattering configuration, the incoming and scattered polarization vectors for the c^* directed nanowire lying along the X axis are given by

$$\hat{e}_{l,s}=\begin{pmatrix} -\sin(\psi_{L,S}) \\ 0 \\ -\cos(\psi_{L,S}) \end{pmatrix}$$

Accordingly, only bands of A_1 symmetry will be sensitive to the phase (as well as the relative magnitudes) of the tensor elements. Writing the two tensor elements involved as $|a|e^{i\phi_a}$ and $|c|e^{i\phi_c}$, the parallel ($\psi_S=\psi_L$)and perpendicular ($\psi_S=\psi_L+90^\circ$) components of the Raman intensity for an A_1 mode obtained from a c^*-directed nanowire will be given by

$$I_{\parallel} \sim |a|^2\sin^4(\psi_L)+|c|^2\cos^4(\psi_L)+\frac{|a||c|}{2}\cos(\phi_{ac})\sin^2(2\psi_L), \tag{2a}$$

$$I_{\perp} \sim \left[\left|\frac{a}{2}\right|^2+\left|\frac{c}{2}\right|^2-\frac{|a||c|}{2}\cos(\phi_{ac})\right]\sin^2(2\psi_L), \tag{2b}$$

where $\phi_{ac}=|\phi_a-\phi_c|$.

Figure 3 summarizes the Raman intensities, shown as polar plots (filled and open circles indicate $\perp$ and $\parallel$ configurations, respectively), of the various bands as a function of ψ_L. (The Raman intensities are proportional to the length of the vector from the origin of the polar plot.) The polarization dependence of the intensities of the various bands in Fig. 3 are, on the whole, consistent with what is expected for a c^*-directed nanowire oriented as shown in Fig. 2. Specifically, the intensity of the E_2^H band is maximum at $\psi_L=90^\circ$ and null at $\psi_L=0^\circ$. $I_\perp$ is also consistent with expectation. The polarization dependence of the intensity of the E_1(TO) mode also accords with expectation except for a nonvanishing background. (The relative intensities calculated as a function of polarization direction for the $\parallel$ and $\perp$ configurations are also shown in Fig. 3). Although for reasons of symmetry we do not expect quasiphonons to form by A_1-E_1 mixing, to first order,[23] the presence of the background might signal their formation probably due to polarization leakage.

The best value of ϕ_{ac} was determined graphically,[4] as is shown in Fig. 4, by comparing the measured Raman intensities determined in the parallel and perpendicular configurations with Raman intensities calculated using Eqs. (2) as a function of ϕ_{ac} and ψ_L. The best fit was determined to be $\phi_{ac}=\pi/2$, for both $\parallel$ and $\perp$ configurations after subtracting a small background from $I_\perp$ that probably arises from depolarization. Since this phase shift depends on the electronic structure and is a manifestation of the frequency dependence of the complex susceptibility,[5] it will depend on the photon energy of the exciting light and on the charge carrier concentration and may therefore vary from nanowire to nanowire. Because all the nanowires studied were fabricated using the same synthetic process,[20] we will assume that the charge carrier concentration is similar in all of them and that we can therefore use the same phase shift throughout this study.

The photoluminescence (PL) spectrum of a bundle of GaN nanowires excited at 300 K by a He-Cd laser operated

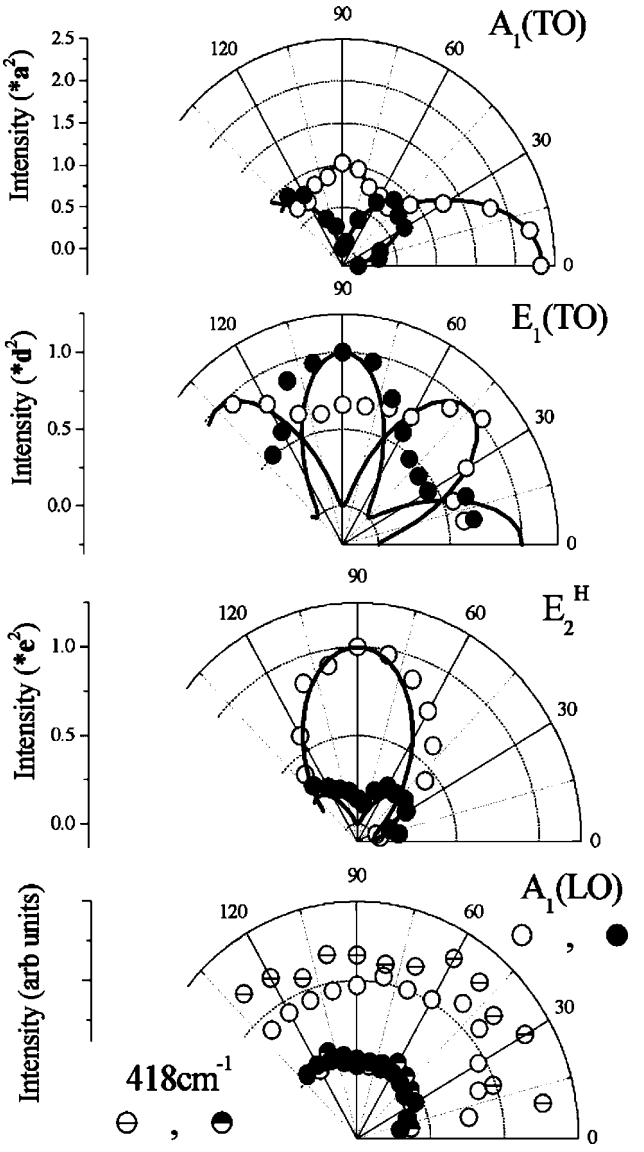

FIG. 3. Polar plots (filled and open circles are for ⊥ and ∥ configurations, respectively), which summarize the Raman intensities of various bands from the c^*—directed nanowire as a function of the angle (ψ_L) between the X axis and the direction of the electric vector of the incident light. Relative intensities calculated as a function of the polarization direction are also shown.

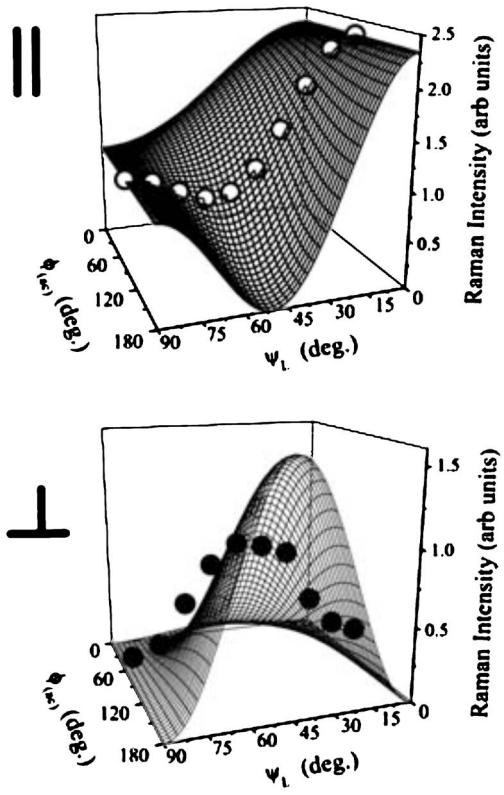

FIG. 4. The best value of $\phi_{ac}=\pi/2$ for both ∥ and ⊥ polarization configurations as determined graphically by comparing the measured Raman intensities (∥ open circles and ⊥ filled circles) with Raman intensities calculated as a function of ϕ_{ac} and ψ_L using Eqs. (2). The best fit was determined after subtracting a small background from $I_\perp$ that probably arises from depolarization.

at 325 nm is shown in Fig. 5. Besides the usual ultraviolet luminescence (UVL) band, two bands are observed in the spectrum: a yellow luminescence (YL) centered at ~2.24 eV and a blue luminescence (BL) at ~2.89 eV. In-gap states due to multiply charged defects are known to exist in GaN. Indeed, the YL has previously been ascribed to transitions from the conduction band or from shallow donor levels into deep n-GaN acceptor defect states such as the acceptorlike gallium vacancy, V_{Ga}.[24] The broad BL observed even at high temperature in undoped GaN is due to transitions from the conduction band to a relatively deep one such as the $V_{Ga}O_N$ acceptor level located ~0.8 eV above the valence band.[24] (O_N is an impurity defect in which oxygen is substituted for nitrogen.)

Photoionization, the inverse process to luminescence, can occur in n-type GaN when an electron from an acceptor level is promoted to the conduction band or to a defect excited state. As a result, the photoluminescence excitation (PLE) spectrum corresponding to a particular PL band is expected to track the absorption spectrum, more or less. This is indeed

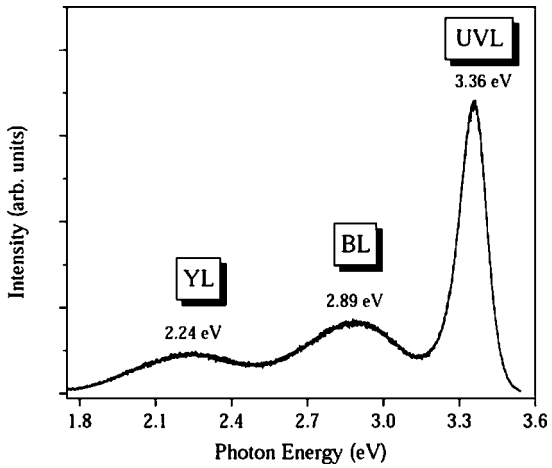

FIG. 5. The photoluminescence (PL) spectrum of a bundle of GaN nanowires excited at 300 K by a He-Cd laser operated at 325 nm.

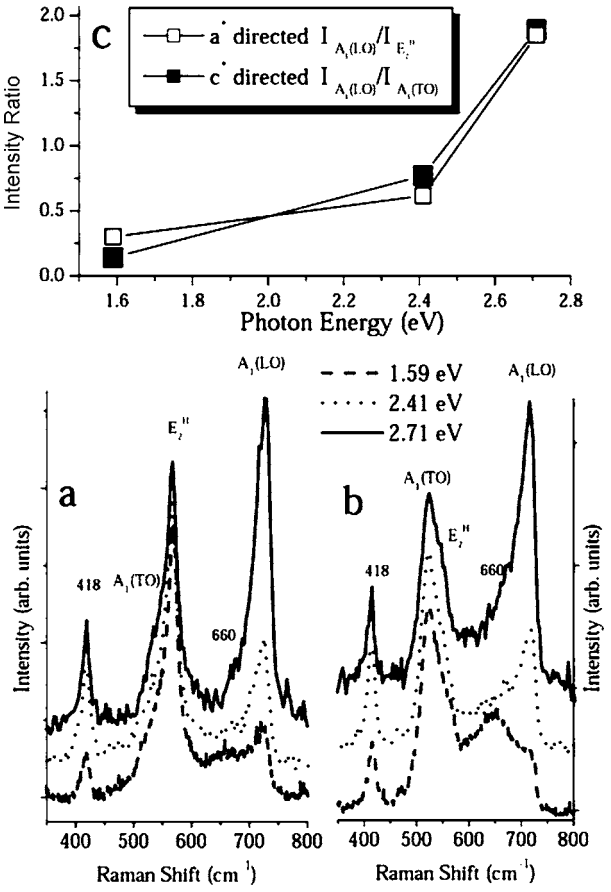

FIG. 6. (a) Raman spectra of a single, a^*-directed nanowire at the excitation energies indicated; (b) same as (a) but for a c^*-directed nanowire; (c) the intensity ratio dependences as a function of excitation energy that clearly show a resonance profile for both nanowires.

what is reported,[25] where only a moderate decrease in the YL intensity of an undoped GaN layer on sapphire was found when the excitation energy was decreased to 2.41 eV, suggesting the coexistence of several defects with similar ionization energies. In a study that compared PL with photoconductivity (PC) and with the resonance Raman profile at room temperature, Chen *et al.*[26] show convincingly that all three effects are correlated and peaked in the same energy range (2.3–2.4 eV), which is associated with the YL deep-acceptor-to-conduction-band transition in the *n*-type GaN epilayer on sapphire.

Significant sub-band-gap absorption was also observed for GaN thin films that were intentionally grown by metal-organic chemical-vapor deposition (MOCVD) to have a high defect density.[27] GaN nanowires that were fabricated using the same synthetic process,[11] and shown to have PL spectrum with significant YL band intensity,[12] were also shown to possess substantial optical absorption coefficients at excitation energies similar to those used in our study.[11]

In summary, the aggregate knowledge gleaned from PL (Refs. 12 and 26), absorption,[11,27] PLE (Ref. 25), PC and resonance Raman spectroscopy,[26] together with the inherent tendency of nanowires to grow with a high concentration of defects as shown convincingly in the PL spectrum (Fig. 5), is

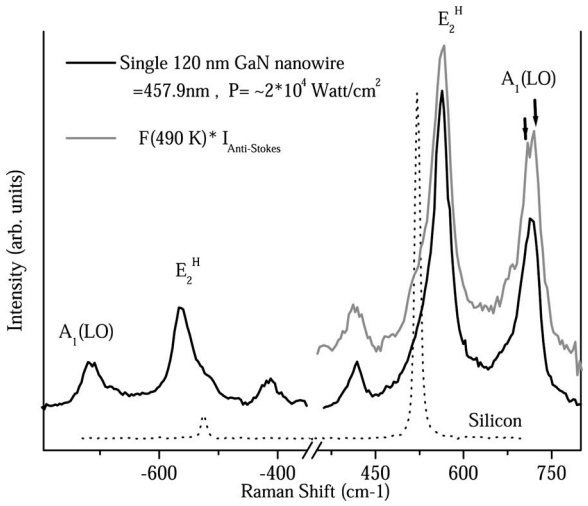

FIG. 7. The complete anti-Stokes and Stokes spectrum for a single 120 nm nanowire excited at a photon energy of 2.71 eV. The spectrum of Silicon (at a similar power density) is included for comparison. For clarity, the anti-Stokes spectrum multiplied by F (490 K) is shown in gray; where $F(T)=[E_l-E_{ph}/E_l+E_{ph}]^4 \exp(E_{ph}/kT)$ (E_l is the incident laser energy and E_{ph} is the phonon energy). This procedure estimates the temperature of the nanowire and indicates the enhancement in the anti-Stokes side of the A_1(LO) mode.

suggested to account for the complex-valued dielectric function observed for GaN in our study even at sub-band-gap photon energies.

A number of consequences arise from this conclusion, such as the expectation of resonancelike profiles for the Raman excitation modes and a possible increase in local temperature due to absorption in the nanowire. Figures 6(a) and 6(b) show the Raman spectra of an a^* and a c^* directed nanowire, respectively. In Fig. 6(b), the Raman spectrum is normalized to the A_1(TO) intensity; while in Fig. 6(a) it is normalized to the E_2^H mode.[28] (The E_2^H mode is not an allowed mode for a c^* nanowire at $\psi_L=0$.) The intensity ratio of these bands to the corresponding A_1(LO) bands [Fig. 6(c)] indicates, for both nanowires, a resonance profile similar to that reported in Ref. 11 for GaN nanowires. This corroborates the presence of absorptions in the wavelength region used and implies the presence of strong electron interaction with the A_1(LO) phonon when excited defects in the GaN nanowire are photoionized.

The presence of nanowire absorption at the laser wavelengths we used in this study also raises the possibility that significant local heating may occur that could lead to nanowire oxidation at somewhat lower temperatures, such as was observed in GaN powders at 900 K.[29] An anti-Stokes-to-Stokes intensity analysis, however, indicates otherwise.

The complete anti-Stokes and Stokes spectrum for a single 120 nm nanowire excited at a photon energy of 2.71 eV is shown in Fig. 7. The spectrum of silicon (at a similar power density) is included for comparison. Even if one discounts the occurrence of laser pumping of vibrationally excited states (which, at any rate, leads to an overestimation of the local temperature), the analysis produces a maximum local temperature ~490 K and 380 K for 2.71 eV

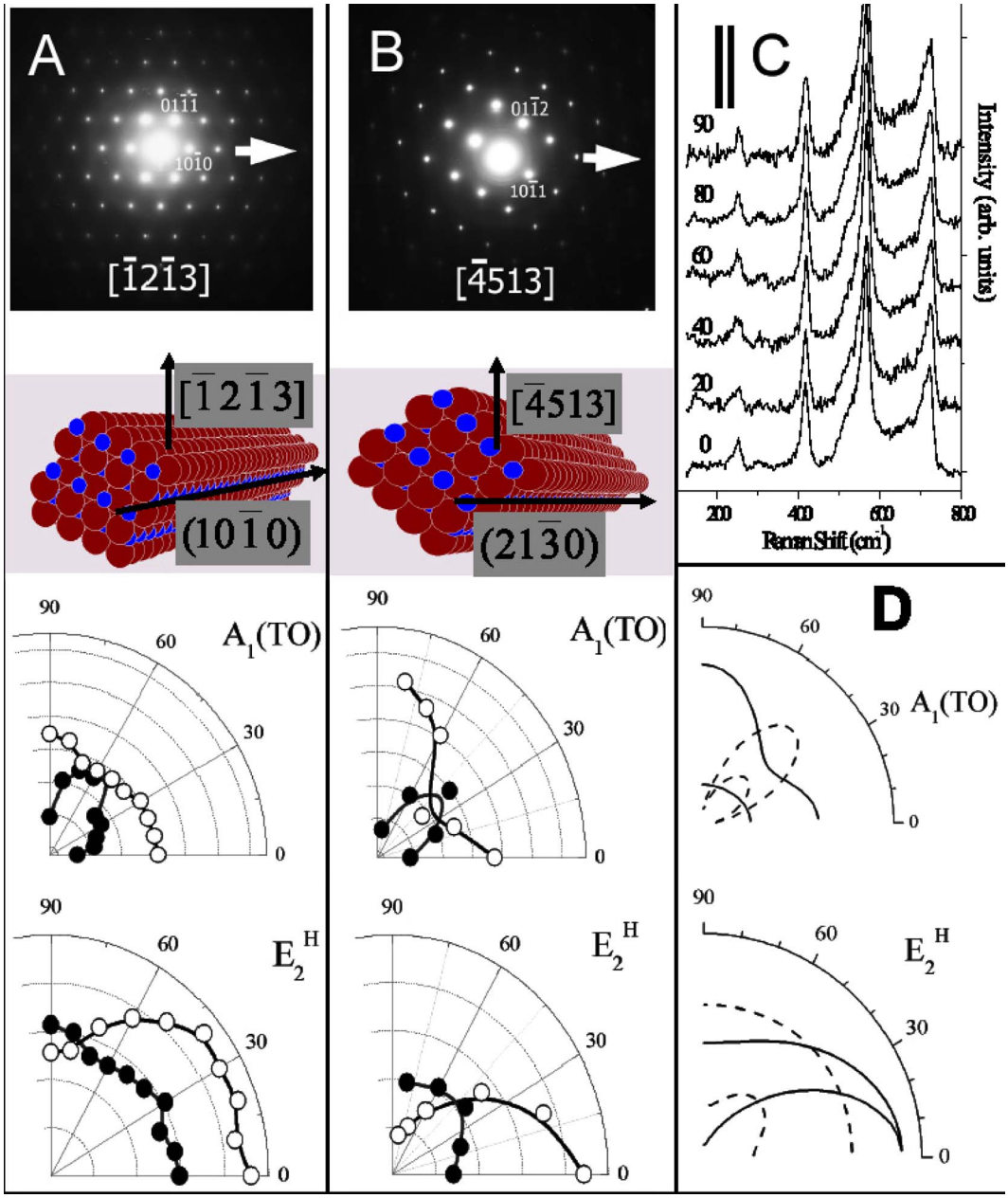

FIG. 8. (Color online) Polar plots of the E_2^H and the A_1(TO) bands for two nanowires. The nanowires shown in (a) and (b), referred to as w_1 and w_2, have ~200 nm and ~150 nm diameters, respectively. Electron diffraction images and the crystallographic disposition of the nanowires deduced from them are also shown. (c) a series of parallel (∥) polarized Raman spectra measured as a function of the polarization direction of the incident light for w_1. (d) a plot the Raman intensity for the E_2^H and A_1(TO) bands calculated for θ=32°, 59° for the ∥ (solid line) and ⊥ (dashed line) configurations (the higher intensities correspond to θ=59°).

and 2.41 eV, respectively. *Prima facie*, this seems too low a temperature for oxidation to occur, a conclusion supported by the electron diffraction image obtained post-laser irradiation, which indicated that the crystalline nature of the nanowire is unchanged.

A noteworthy result is that the A_1(LO) band is enhanced by ~10–15% in the anti-Stokes spectrum with a clear separation between the bands at 724 cm^{-1} and 710 cm^{-1}.[30] The observed asymmetry in the phonon intensity for the anti-Stokes and Stokes spectra likely comes about as a result of differing resonance conditions for the incident and scattered photons with the material's electronic transitions—another manifestation of the resonance nature of the process in circumstances when the electron-phonon interaction with the A_1(LO) mode is strongly E_1 dependent. The observations suggest that the resonance in the anti-Stokes region is better than in the Stokes region of the spectrum.[31]

In addition to the phase, the analysis of the A_1(TO) mode intensity yielded the ratio $|c/a|=1.53$ as compared with $|c/a|=2.11$ reported for GaN thin films deposited on sapphire (also measured with at 514.5 nm).[32] The origin of this reduced anisotropy is uncertain. It may be due to differences in the strain sustained by the nanowire and thin film resulting either from their differing surface-to-volume ratios or the

different growth mechanism used to produce the two sets of samples.

An interesting observation is the significant intensity of the A_1(LO) mode (Fig. 2), which should be silent for c^*-directed nanowires, as is indeed the case for GaN thin films.[6] In fact, the A_1(LO) mode is comparable in intensity to the A_1(TO) mode. However, their polarization dependences differ greatly. The intensity of the A_1(LO) mode is almost independent of ψ_L. The center band frequency of the A_1(LO) mode of the nanowire is also redshifted by ~ 8 cm^{-1} from its position in the spectrum of thin films. Additionally, the band is found to have a second component (at ~ 710 cm^{-1}) whose polarization dependence is similar to that of the main band.[33] Since high-resolution transmission electron microscopy (HR-TEM) and electron diffraction analyses indicate the nanowires to be good quality crystals and that the frequency shift is independent of diameter (it was observed even for large-diameter nanowires), we exclude quantum confinement as a possible cause both of the frequency shift and the appearance of the A_1(LO) mode, as was previously suggested.[11] Shifts of this magnitude, however, have been reported for highly strained pyramids.[34] The effect of strain on the electronic properties of nanowires induced during growth has also been reported.[13]

Because an a^*-directed nanowire lacks the cylindrical symmetry of its c^*-directed counterpart, its polarized Raman intensities will depend both on the angle subtended by the incident polarization vector relative to the nanowire's axis as well as on the angle between the c axis (which is transverse to the long axis of the nanowire) and the normal to the surface on which the nanowire is laid. In Figs. 8(a) and 8(b), we compare the polar plots for the E_2^{H} and the A_1(TO) bands for two (~ 200 nm and ~ 150 nm diameter, respectively) nanowires with their electron diffraction patterns which are also shown. (The nanowires depicted in Figs. 8(a) and 8(b) will be referred to as w_1 and w_2, respectively. The TEM image of nanowire w_2 is shown in Fig. 1). The diffraction results corroborate the fact that both nanowires are either a^* directed (w_1) or (in the case of w_2) are grown normal to the $(21\bar{3}0)$ plane, a direction which is within 19.2° to a^*. The analysis of the electron diffraction results indicate that for the two nanowires the normal to the (laboratory-fixed) surface on which they lie correspond to the $[\bar{1}2\bar{1}3]$ and the $[\bar{4}513]$ directions, respectively, for w_1 and w_2. This means that the c axes of the two nanowires are inclined, respectively, at 31.9° and 58.7° from the normal. These crystalline orientations are shown schematically in Figs. 8(a) and 8(b).

Figure 8(c) shows a series of parallel (∥) polarized Raman spectra measured as a function of the polarization direction of the incident light for nanowire w_1. The contrast with the analogous spectra shown in Fig. 2 for a c^*-directed nanowire is evident. Specifically, for the a^*-directed nanowire, the E_2^{H} and A_1(TO) spectral features do not change significantly with polarization angle. [Recall that for the c^*-directed nanowire the E_2^{H} mode is null when the A_1(TO) is maximal.] Particularly for the measurements shown in Fig. 8, the intensities of the nanowires showed some fluctuations from measurement to measurement likely due to drift in the position of the nanowire in the diffraction-limited spot during the long measurement time, which could be up to 8 min. Such drift would change both the intensity of the Raman band and the background proportionately. To circumvent the effect of drift, we normalized all the measurements to the polarization-insensitive background signal for each measurement. That the Raman background intensity is independent of ψ_L, and hence a good intensity normalization property, was inferred from the fact that for measurements on single nanowires with comparable dimensions (~ 150–200 nm) placed on an alumina disk, which showed very little intensity drift with time, the intensity of the background was found to be virtually independent of ψ_L.

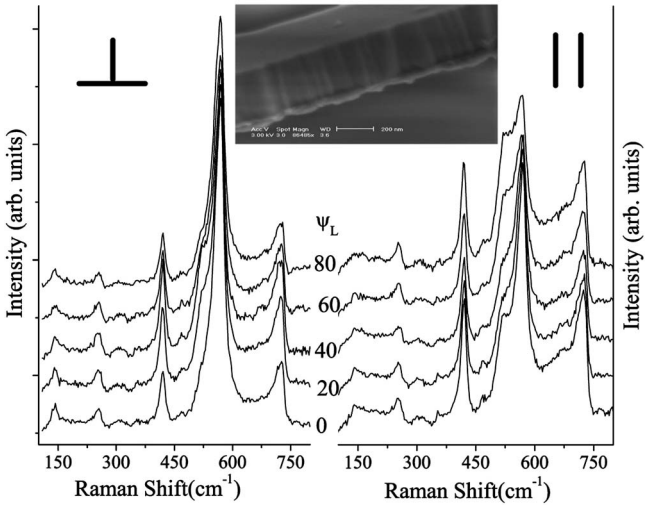

FIG. 9. A series of parallel (∥) and perpendicularly (⊥) polarized Raman spectra measured as a function of the polarization direction of the incident light for a ~ 300 nm diameter nanowire [as determined by scanning electron microscopy (SEM)] with unknown crystallographic orientation.

The sensitivity of the measurement to the angle of inclination of the c axis is the prominent factor that dictates the different polarization behavior of w_1 and w_2. We first consider the E_2^{H} band. In Fig. 8(d) we plot the polarization dependence of the Raman intensities of the E_2^{H} and A_1(TO) bands for $\theta = 32°$ and 59° for the ∥ (solid line) and the ⊥ (dashed line) configurations. (The higher intensities correspond to $\theta = 59°$.) The calculated and the experimental angle-dependent intensity profiles for the two nanowires are in good agreement. While both nanowires have comparable intensities in the parallel configuration, when the E vector is directed perpendicular to the long the axis of nanowire, the signal decreases with increasing θ [the inclination of the c axis with respect to the normal to the (laboratory-fixed) surface] since the susceptibility tensor of the E_2^{H} mode has no z-subscripted components.

The A_1(TO) mode analysis is more complicated since, for it, one needs to consider two factors that are not relevant for the E_2^{H} band: (1) the TO mode intensity is reduced as the normal become tilted away from the $[\bar{1}2\bar{1}0]$ axis at the expense of an increased LO mode intensity,[23] and (2) quasiphonons with ill-defined symmetry properties can arise whose frequencies lie between those of the A_1(TO) and E_1(TO) modes.[23] The two effects are not easy to decouple.

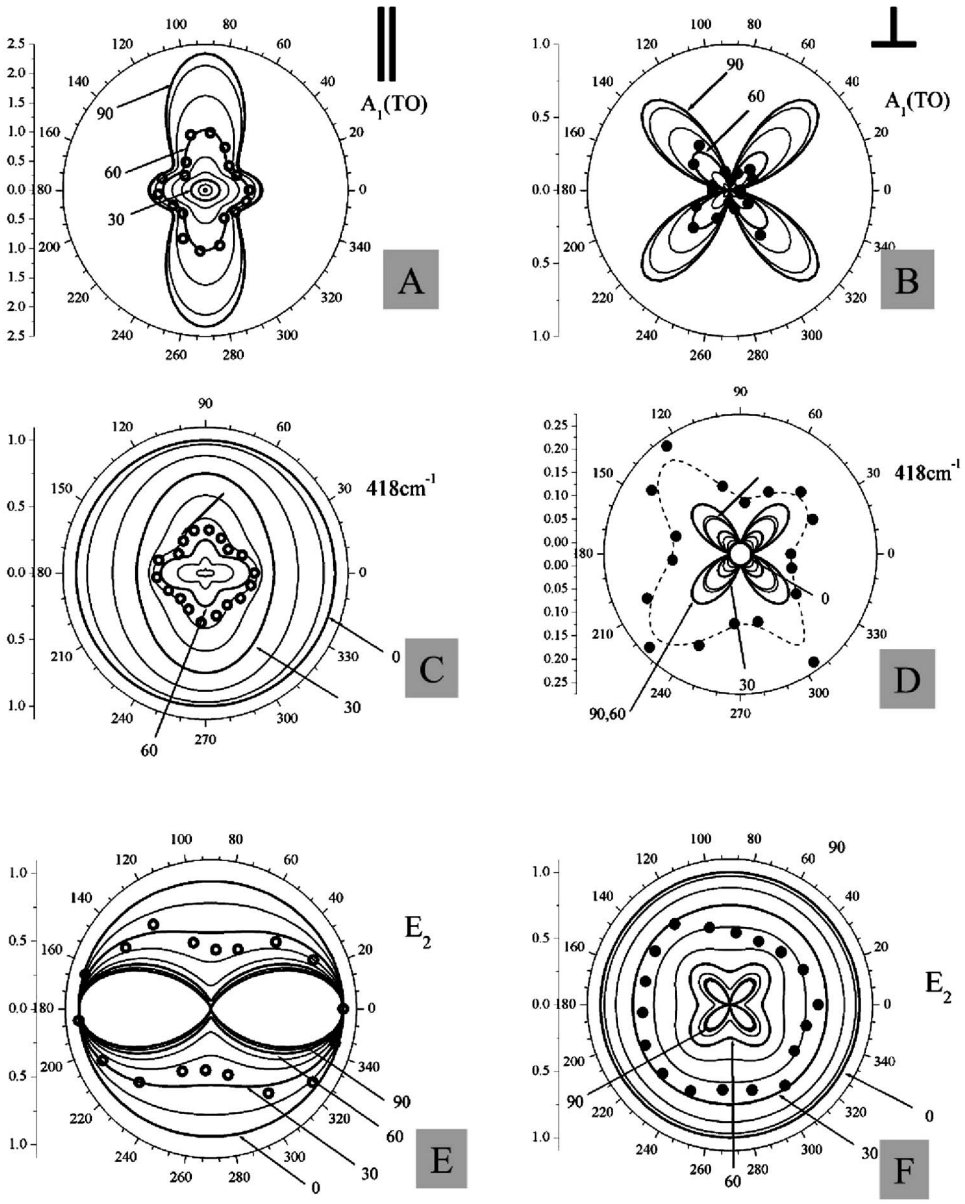

FIG. 10. Polar plots (filled and open circles are for ⊥ and ∥ configurations, respectively), summarizing the Raman intensities of various bands as a function of ψ_L, the angle between the X axis and the direction of the electric vector of the incident light, for the nanowire shown in Fig. 9. Also shown are relative intensities calculated for values of θ calculated in 10° intervals with the contours corresponding to θ=90, 60, 30, and 0 degrees emphasized by using thicker lines.

Despite these limitations, and although the E_2^H dependence is the more reliable, the different polarization angle dependence of the A_1(TO) bands of the two a^*-directed nanowires can be understood qualitatively by referring to the simulated polarization angle dependence shown in Fig. 8(d).

When the nanowire diameter was much less than the wavelength of the illuminating light, one can show that the field internal to the nanowire is attenuated with respect to the external field value for field components perpendicular to the long axis of the nanowire.[35] This arises from the continuity relationships on the tangential electric field component and normal electric displacement components of the field. Recent Raman measurements on CuO nanorods with average diameters of 65 nm (Ref. 19) showed that the intensities of all Raman bands were essentially independent of the symmetry properties of the associated tensors but determined solely by the magnitude of the electric field component along the nanowire's long axis. That is, the intensities of all bands had a $\cos^2 \psi_L$ dependence. Highly anisotropic properties were also found in the context of photoluminescence[36,37] and photoconductivity[36] for InP (10–50 nm) (Ref. 36) and Si (18 nm) (Ref. 37). For the nanowires used in this study with diameters in the range 150–200 nm (Fig. 8), the Raman intensities were found to be almost totally determined by the tensor symmetries of the individual bands and very little affected by the reduced dimensions of the nanowire. This is probably due to their larger diameters. It is nevertheless surprising that these quasi-one-dimensional effects would be so significantly reduced at ~150 nm.

We are now in a position to attempt to determine the crystalline orientation and relative disposition of a nanowire whose structure was not previously determined by TEM. Figure 9 shows the Raman spectra obtained for a ~300 nm diameter nanowire deposited on a quartz substrate. The overall polarization dependence of the intensities of the various bands is consistent with an a^*-directed nanowire. The intensity of the E_2^H band for the ∥ configuration decreases as ψ_L increases from 0° to 90°. The intensities of the A_1(TO) and

A_1(LO) modes oscillate with increasing ψ_L but with opposite phase; and the E_1(TO) intensity is not very sensitive to polarization. What remains to be determined is angle, θ, the inclination of the c axis with respect to the normal to quartz substrate. Figures 10(a) and 10(b) show a series of contours depicting the expected polarization dependence of the $\parallel$ and $\perp$ components, respectively, of the A_1(TO) mode as a function of ψ_L for θ=0–90°. With $\theta \sim 55°$, a good fit is obtained for both components of the A_1(TO) mode. In Figs. 10(c) and 10(d), the same procedure is shown for the 418 cm^{-1} modes, which behave similarly to the A_1(LO) mode. Its $\parallel$ component fits a contour calculated with a similar value of θ. The calculated angle-dependent polarization contours are determined using a deformation potential that for the A_1(LO) phonons does not include the term that is proportional to the electro-optic coefficient. This term arises from the electron-phonon interaction caused by the macroscopic electric field carried by LO phonons potentially greatly affecting the scattering efficiency. It may also alter the polarization dependence of the intensity of this band.[23] The fact that the agreement is good for the $\parallel$ component suggests that the contribution of the electro-optical mechanism is sufficiently isotropic (as is the case for the c^*-directed nanowire; see Fig. 3) to cause the polarization properties of this band to retain the oscillatory behavior observed. It is probable that in the $\perp$ configuration, the A_1(LO) mode, that according to the calculations should show much lower intensities [Fig. 8(d)], is more sensitive to this component and therefore has a more isotropic background.

This rather consistent pictured is marred a little by the fact that the polarization dependence observed for the E_2^H band [Figs. 10(e) and 10(f)] fits best to the contour calculated for $\theta \sim 40°$, although the fit is not nearly as good as for the two previously discussed bands. Hence, rather than concluding that we have successfully determined θ to within ±5° of ~60°, we must expand the uncertainty by approximately a factor of 3. Nevertheless, we have shown that Raman was able to choose unequivocally between a c^*-directed and an a^*-directed nanowire, and in the case of the latter, determine its orientation with respect to laboratory-fixed coordinates within tolerable limits.

IV. CONCLUSIONS

By investigating the polarization dependence of the Raman intensities of the observed bands as a function of the angle between the long axis of the single GaN nanowires and the electric vector of the incident (and scattered) light, one is able to distinguish between growth in the a^* direction and c^* direction. Furthermore, the sensitivity of the Raman spectrum to the relative orientation of the k vector with respect to the crystallographic direction, which coincides with the surface normal, was also shown. Simultaneous TEM analyses confirm the conclusions derived from the Raman measurements.

The variable polarization angle Raman intensities at the wavelength used (514.5 nm) for the A_1(TO) phonon could only be understood if one assumed a complex-valued Raman tensor. The measurements allowed us to determine the relative phase between the χ_{xx} and χ_{zz} susceptibility components, which turned out to be $\sim \pi/2$ for the nanowires used in this study.

The detection of resonance enhancement together with the tendency of the nanowires to grow with a high concentration of defects and the observation of yellow luminescence in the PL spectrum may account for the complex-valued Raman tensor we observe for GaN even at sub-band-gap photon energies. This resonant shape to the excitation profiles also leads to an increase in the local temperature as indicated by an anti-Stokes-to-Stokes intensity analysis on the single 120 nm nanowire measured at ~490 K and 380 K for 2.71 eV and 2.41 eV, respectively.

ACKNOWLEDGMENTS

M.M. is grateful to the Canadian Institute for Advanced Research for support. We are also grateful to the Institute for Collaborative Biotechnologies for support through Grant No. DAAD19-03-D-0004 from the U.S. Army Research Office and to the Air Force Office of Scientific Research under DURINT Grant No. F49620-01-1-0459. This work made extensive use of the MRL Central Facilities at UCSB supported by the MRSEC Program of the National Science Foundation under Grant No. DMR-0080034.

*Corresponding author. On leave from: Department of Physical Chemistry, Nuclear Research Center, Negev, P.O. Box 9001, Beer-Sheva 84190, Israel. Electronic address: T.Livneh@nrcn.org.il

†Corresponding author. Electronic address: mmoskovits@ltsc.ucsb.edu

[1] Y. Huang, X. Duan, Y. Cui, and C. M. Lieber, Nano Lett. **2**, 101 (2002).

[2] Y. Huang, X. Duan, Q. Wei, and C. M. Lieber, Science **291**, 630 (2001).

[3] J. C. Johnson, H.-J. Choi, K. P. Knusten, R. D. Schaller, P. Yang, and R. J. Saykally, Nat. Mater. **1**, 106 (2002).

[4] T. Strach, J. Brunen, B. Lederle, J. Zegenhagen, and M. Cardona, Phys. Rev. B **57**, 1292 (1998).

[5] E. T. Heyen, S. N. Rashkeev, I. I. Mazin, O. K. Anderson, R. Liu, M. Cardona, and O. Jepsen, Phys. Rev. Lett. **65**, 3048 (1990).

[6] H. Harima, J. Phys.: Condens. Matter **14**, R967 (2002).

[7] L. Bergman, M. Dutta, and R.J. Nemanich, in *Raman Scattering in Material Science*, edited by W. H. Weber and R. Merlin (Springer, New York, 2000), p. 273.

[8] V. Y. Davydov, Y. E. Kitaev, I. N. Goncharuk, A. N. Smirnov, J. Graul, O. Semchinova, D. Uffmann, M. B. Smirnov, A. P. Mirgorodsky, and R. A. Evarestov, Phys. Rev. B **58**, 12899 (1998).

[9] H. Siegle, G. Kaczmarczyk, L. Filippidis, A. P. Litvinchuk, A. Hoffmann, and C. Thomsen, Phys. Rev. B **55**, 7000 (1997).

[10] T. Azuhata, T. Sota, K. Suzuki, and S. Nakamura, J. Phys.: Condens. Matter **7**, L129 (1995).

[11] H.-L. Liu, C.-C. Chen, C.-T. Chia, C.-C. Yeh, C.-H. Chen, M.-Y. Yu, S. Keller, and S. P. DenBaars, Chem. Phys. Lett. **345**, 245 (2001).
[12] C.-C. Chen, C.-C. Yeh, C.-H. Chen, M.-Y. Yu, H.-L. Liu, J.-J. Wu, K.-H. Chen, L.-C. Chen, J.-Y. Peng, and Y.-F. Chen, J. Am. Chem. Soc. **123**, 2791 (2001).
[13] H. W. Seo, S. Y. Bae, J. Park, H. Yang, K. S. Park, and S. Kim, J. Chem. Phys. **116**, 9492 (2002).
[14] S. Piscanec, M. Cantoro, A. C. Ferrari, J. A. Zapien, Y. Lifshits, S. T. Lee, S. Hofmann, and J. Robertson, Phys. Rev. B **68**, 241312(R) (2003).
[15] R. Gupta, Q. Xiong, C. K. Adu, U. J. Kim, and P. C. Eklund, Nano Lett. **3**, 627 (2003).
[16] R. Gupta, Q. Xiong, G. D. Mahan, and P. C. Eklund, J. Nanosci. Nanotechnol. **3**, 1745 (2003).
[17] M. S. Dresselhaus G. Dresselhaus, A. Jorio, A. G. Souza Filho, M. A. Pimenta, and R. Saito, Acc. Chem. Res. **35**, 1070 (2002).
[18] G. S. Duesberg, I. Loa, M. Burghard, K. Syassen, and S. Roth, Phys. Rev. Lett. **85**, 5436 (2000).
[19] T. Yu, X. Zhao, Z. X. Shen, Y. H. Wu, and W. H. Su, J. Cryst. Growth **268**, 590 (2004).
[20] G. S. Cheng, A. Kolmakov, Y. X. Zhang, R. Munden, M. Reed, G. Wang, D. Moses, and J. P. Zhang, Appl. Phys. Lett. **83**, 1578 (2003).
[21] K. Mizoguchi and S. Nakashima, J. Appl. Phys. **65**, 2583 (1989).
[22] P. Perlin, J. Camassel, W. Knap, T. Taliercio, J. C. Chervin, T. Suski, I. Grzegory, and S. Porowski, Appl. Phys. Lett. **67**, 2524 (1995).F. Demangeot, J. Frandon,M. A. Renucci, C. Meny, O. Briot, and R. L. Aulombard, J. Appl. Phys. **82**, 1305 (1997).
[23] C. A. Arguello, D. L. Rousseau, and S. P. S. Porto, Phys. Rev. **181**, 1351 (1969).
[24] M. Reshchikov and H. Morkoç, J. Appl. Phys. **97**, 061301 (2005).
[25] E. Calleja, F. J. Sánchez, D. Basak, M. A. Sánchez-García, E. Muñoz, I. Izpura, F. Calle, J. M. Tijero, L. Sánchez-Rojas, B. Beaumont, P. Lorenzini, and P. Gibart, Phys. Rev. B **55**, 4689 (1997).
[26] H. M. Chen, Y. F. Chen, M. C. Lee, and M. S. Peng, Phys. Rev. B **56**, 6942 (1997).
[27] O. Ambacher, W. Rieger, P. Ansmann, H. Angeher, T. D. Moustakas, and M. Stutzmann, Solid State Commun. **97**, 365 (1996).
[28] The A_1(TO) and the E_2^H modes have similar E_1 dependence. We note that for the *n*-type GaN epitaxial film (Ref. 26) resonance enhancement was found for the A_1(LO) and E_2^H bands [the A_1(TO) is not allowed in the measured configuration]. However, it is clear that for GaN nanowires the A_1(LO) mode intensity has the stronger E_1 dependence. This E_1 dependence is even more pronounced if we consider a resonant nature of the band with respect to which it was normalized.
[29] C. Tang, Y. Bando, and Z. Liu, Appl. Phys. Lett. **83**, 3177 (2003).
[30] H. D. Li, S. L. Zhang, H. B. Yang, G. T. Zou, Y. Y. Yang, K. T. Yue, X. H. Wu, and Y. Yan, J. Appl. Phys. **91**, 4562 (2002).
[31] Peter Y. Yu and M. Cardona, *Fundamentals of Semiconductors* (Springer-Verlag, Berlin, 1999), p. 390.
[32] I. Loa, S. Gronemeyer, C. Thomsen, O. Ambacher, D. Schikora, and D. J. As, J. Raman Spectrosc. **29**, 291 (1998).
[33] We consider unlikely the attribution of these bands to surface optical (SO) phonons as suggested in Ref. 30. The Raman spectrum from a single wire immersed in an index matching fluid with dielectric constant of ε_m=2.19 showed a ~3 cm^{-1} shift (relative to the spectrum taken at ambient conditions), of the 724 and 710 cm^{-1} bands. According to calculations (Ref. 16), if these bands were attributed to SO phonons, an increase in ε_m of the surrounding medium from 1 to 2.19 is expected to lead to about order of magnitude higher shifts.
[34] R. Fornari, M. Bosi, D. Bersani, P. P. Lottici, and C. Peloci, Semicond. Sci. Technol. **16**, 776 (2001).
[35] L. D. Landau, E. M. Lifshitz, and L. P. Pitaevskii, *Electrodynamics of Continuous Media* (Pergamon, Oxford, 1984), pp. 34–42.
[36] J. Wang, M. S. Gudiksen, X. Duan, Y. Cui, and C. M. Lieber, Science **293**, 1455 (2001).
[37] J. Qi, A. M. Belcher, and J. M. White, Appl. Phys. Lett. **82**, 2616 (2003).